Fluorescence Quenching in Electron-Donating Solvents. 1. Influence of the Solute−Solvent Interactions on the Dynamics

Ana Morandeira, Alexandre Fürstenberg, Jean-Claude Gumy,† and Eric Vauthey*

Department of Physical Chemistry, University of Geneva, CH-1211 Geneva, Switzerland

Received: February 6, 2003; In Final Form: May 12, 2003

The electron transfer (ET) quenching dynamics of excited perylene (Pe), cyanoperylene (PeCN), methanolperylene (PeOH), and methylperylene (PeMe) in *N*,*N*-dimethylaniline (DMA) has been investigated using ultrafast fluorescence up-conversion. Measurements of the rotational dynamics of PeCN and PeMe in nonpolar and polar inert solvents using optically heterodyned polarization spectroscopy are also presented. The fluorescence decay in DMA is strongly nonexponential and about 10 times faster with PeCN than with the other electron acceptors. The quenching dynamics has been analyzed with a model distinguishing three types of donor molecules surrounding the acceptor: those with optimal orientation for ET and those requiring orientational or translational diffusion prior to ET. According to this model, which can account for the whole fluorescence decay, the faster quenching dynamics of PeCN is not due to a larger ET rate constant, but to a larger number of donor molecules, typically three to four, with an optimal orientation. This is explained by the effect of dipole−dipole interaction between PeCN and the donor molecules, which favors mutual orientations with a large electronic coupling. With the other acceptors, this interaction is either not present or does not lead to ET active geometries. The occurrence of this interaction is substantiated by the rotational dynamics measurements.

Introduction

A major difficulty when investigating bimolecular photoinduced electron-transfer (ET) reactions in solution is the determination of the intrinsic ET rate constant, k_{ET}. Indeed, diffusional encounter must first take place before the reaction can occur. Therefore, as soon as ET is faster than this initial step, the observed rate constant is that of diffusion and no information on the actual ET dynamics can be obtained. This outcome has been clearly demonstrated in the famous ET quenching experiments of Weller and co-workers.[1] For example, in acetonitrile, the quenching rate constant k_q becomes equal to the diffusional rate constant ($k_{dif} \approx 2 \times 10^{10}$ M^{-1} s^{-1}) as soon as the ET driving force, ΔG_{ET}, becomes more negative than about −0.2 eV. It is therefore essentially impossible to test the predictions of ET theories with these bimolecular ET reactions. There have been mainly two approaches to circumvent this limitation and to access k_{ET} above the diffusion limit:

(1) The analysis of the transient effect.[2−7] There is always a fraction of the excited reactant population with a quencher molecule at a distance where ET can occur without significant diffusion. Therefore, this subpopulation is quenched with a time constant essentially equal to k_{ET}. The remaining population has no neighbor quencher, and thus, diffusion is required before quenching. As a result, the decay of the excited population is nonexponential, and at early time, the quenching rate is time dependent. This transient effect is very general and can be easily observed by time-resolved fluorescence spectroscopy, provided good time resolution and sensitivity. To extract k_{ET} from such data, the Collins−Kimball model is used in most cases.[2,4,5,8] From this analysis, which requires the knowledge of the diffusion coefficient of the reactants, a radius of the reaction sphere and a rate constant for the quenching in this volume are obtained. Although this analysis is rather straightforward, the interpretation of the output parameters of this model, which considers the reacting molecules as spheres and the solvent as a continuum, is not so clear. This concerns especially the radius of the reaction sphere, which is usually interpreted as the ET distance. This distance has been observed to increase markedly with the driving force and the solvent viscosity, and ET distances as large as 14 Å have been reported in acetonitrile.[2,9]

(2) ET in reacting solvents. This approach has been pioneered by Yoshihara and co-workers, who have intensively investigated the ultrafast ET quenching dynamics of fluorescent electron acceptors, like coumarins and ionic dyes, in electron-donating solvents, and in particular in aniline derivatives.[10−13] In these systems, the fluorescence quenching was found to be ultrafast and to occur in a time scale shorter than that of diffusional solvation. Similar ultrafast ET quenching processes in electron-donating solvents have then been reported by other groups.[14,15] In these studies, the ET rate constant was assumed to be equal to the quenching rate constant, and therefore, bimolecular ET time constants as short as ∼50 fs have been reported.[11,14] This result is very important because it indicates that ET can occur in a time scale comparable to that of vibrational relaxation and even that of electronic dephasing. This opens a very interesting perspective on the possible control of the ET dynamics by the excitation field.[16−19] However, it was shown more recently that the extraction of k_{ET} from such experiments in electron-donating solvents might not be so straightforward. Indeed, molecular dynamics simulations indicate that an excited acceptor of the size of a coumarin can be surrounded by as much as 20 donor molecules.[20] This implies that there might be many possible ET quenching pathways and that the measured quenching rate constant, k_q, may be substantially larger than the rate constant

* To whom correspondence should be addressed. E-mail: eric.vauthey@chiphy.unige.ch.

† Present address: Nestlé Suisse SA, CH-1350 Orbe, Switzerland.

10.1021/jp0343133 CCC: $25.00
Published on Web 06/21/2003

CHART 1

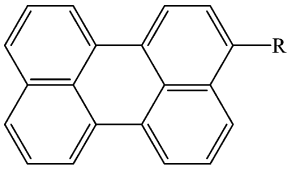

Pe: R=H
PeCN: R=CN
PeOH: R=MeOH
PeMe: R=Me

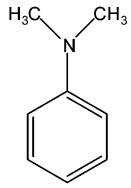

DMA

TABLE 1: Electron Acceptor Properties: Fluorescence Lifetime without Quencher, τ_{fl}, Reduction Potential, E_{red}, Excited-State Energy, $E(S_1)$, ET Driving Force in Polar and Weakly Polar Solvents, ΔG_{ET}, Calculated Using the Weller Expression[24] and with E_{ox}(DMA) = 0.70 V vs SCE[25]

acceptor	τ_{fl}[a] (ns)	E_{red} (V vs SCE)	$E(S_1)$[a] (eV)	$\Delta G_{ET}(\epsilon = 37.5)$ (eV)	$\Delta G_{ET}(\epsilon = 5)$ (eV)
Pe	4.4	−1.66[b,c]	2.8	−0.44	−0.13
PeCN	4.6	−1.36[b]	2.6	−0.54	−0.22
PeOH	4.2	−1.67[c]	2.8	−0.43	−0.13
PeMe	3.7	−1.66[c]	2.8	−0.44	−0.13

[a] In chlorobenzene. [b] In acetonitrile. [c] In THF.

associated with a single ET pathway, k_{ET}. Castner et al., combining fluorescence up-conversion measurements and molecular dynamics simulations, argued that although the number of surrounding solvent molecules is large, the number of molecules having the right orientation and distance for ET is much smaller, of the order of 1−3.[21] Baigar et al. have recently shown that the intramolecular ET rate constant in a covalently linked donor/acceptor pair was close to the largest quenching rate constant measured in an electron-donating solvent, suggesting that in the latter case, the number of active surrounding molecules is small.[22]

The electron donor being the solvent, a moderately polar solvent in the case of anilines, the mutual orientation of the ET reactants, hence the number of active solvent molecules, can be expected to depend markedly on the nature of the solute−solvent interaction. Coincidentally, all the electron acceptors used in the aforementioned experiments are either very polar, like the coumarins,[23] or ionic, like Nile blue, Oxazine 1, and Rhodamine 6G.

We present here our investigation of the influence of solute−solvent interactions on the quenching dynamics of perylene derivatives in an electron-donating solvent, *N*,*N*-dimethylaniline (DMA). The electron acceptors are shown in Chart 1, and their properties relevant to ET quenching are listed in Table 1.

Perylene being nonpolar, the major interaction in DMA is the dispersion interaction. Cyanoperylene has a permanent electric dipole moment of about 4 D, in both S_0 and S_1 states, and therefore, dipole−dipole interaction should be operative in DMA. Finally, methanolperylene is also polar but can additionally make H-bond with DMA.[26]

The ET quenching dynamics was measured using fluorescence up-conversion. As the dipole moment of cyanoperylene does not vary upon excitation, the S_1-S_0 absorption and emission bands of this molecule do not exhibit any solvatochromism due to dipole−dipole interaction. Therefore, to establish that this interaction is indeed operative, the reorientational dynamics of cyanoperylene and methylperylene was investigated in series of nonpolar and polar nonreacting solvents using optically heterodyned polarization spectroscopy.

Experimental Section

Time-Resolved Measurements. The fluorescence lifetime of perylene and perylene derivatives in inert solvents was determined by time-correlated single photon counting (TCSPC). The TCSPC setup is similar to that described in ref 27, except that excitation was performed at 395 nm with a pulsed laser diode (Picoquant model LDH-P-C-400B). The average power at 20 MHz was 0.5 mW, and the pulse duration around 65 ps. The full width at half-maximum of the instrument response function was less than 200 ps.

The fluorescence up-conversion setup has been described in ref 28. Excitation was performed at 400 nm, using the frequency-doubled output of a Kerr lens mode-locked Ti:Sapphire laser (Tsunami, Spectra-Physics). The output pulses between 800 and 840 nm had a duration of 100 fs and a repetition rate of 82 MHz. The pump intensity on the sample was around 10^{14} photons·cm^{-2}·pulse^{-1}. The polarization of the pump pulses was at magic angle relative to that of the gate pulses at 800 nm. The full width at half-maximum (fwhm) of the instrument response function was 210 fs. No significant degradation of the samples was observed after the measurements.

For the optically heterodyned polarization spectroscopy (OHPS) measurements,[29] a fraction of the frequency doubled output of a standard 1 kHz amplified Ti:Sapphire system (Spectra-Physics) was used. The pulses at 400 nm with a duration of 100 fs and an energy of 3 μJ were split in two parts using a 90% transmission beam splitter. The transmitted pulses were used as pump pulses and were focused on the sample with a 90 mm achromatic lens after having passed through a combination of Glan-Taylor polarizer and half-waveplate. The reflected pulses, the probe pulses, were sent along an optical delay line (Physik Instrument) before passing through a Glan-Taylor polarizer, the 90 mm achromatic lens, the sample, and a second Glan-Taylor polarizer (the analyzer). The polarization of the pump pulses was oriented at 45° relative to that of the probe pulses. The crossing angle between the pump and probe beams after the lens was around 3°. The transmitted light was recollimated with a 90 mm lens and its intensity was detected with a photomultiplier tube (Hamamatsu R928), whose output was digitized by a computer board (Axiom AX5210). The extinction ratio of the pair of probe polarizers with sample and lens was better than 5×10^{-6}. For heterodyning, a local oscillator (LO) was realized by rotating the analyzer by 1° from the position of maximum extinction.[30,31] In this case, the LO is in phase with the signal originating from the transient dichroism of the sample. The transmitted light contains contributions from the homodyne signal, the LO and the heterodyne signal. To remove the first two contributions, the measurement has to be repeated with a LO out of phase with the transient dichroism signal.[32,33] In general, this is realized by rotating the analyzer by −1° from the position of maximum extinction. Instead, we preferred to keep the analyzer at +1° and to rotate the polarization of the pump pulses by 90°. With this procedure, the LO remains constant and the phase of the transient dichroism field is shifted by 180°. Subtraction of the out-of-phase signal from the in-phase one results to a time profile that contains only the temporal variation of the heterodyne intensity. A few ps after excitation, the latter is given by[32,34]

$$I_H(t) \propto P(t) \cdot r(t) \qquad (1)$$

where $P(t)$ is the time dependence of the population absorbing at the probe wavelength, in the present case the ground-state

population, and $r(t)$ is that of the polarization anisotropy. During the first few ps, I_H may also contain contributions from the imaginary part of the third order nonlinear susceptibility of the sample, especially of the solvent. Moreover, some ultrafast spectral dynamics, essentially related to solvation, may occur as well.[35,36]

Steady-State Measurements. UV−vis absorption spectra were recorded on a Cary 50 spectrophotometer, and emission spectra were measured with a Cary Eclipse fluorometer.

Samples. Perylene (Pe) was recrystallized in benzene before use. 3-Cyanoperylene (PeCN) and 3-methylperylene (PeMe) were synthesized according to the literature[37] and were purified by column chromatography. 3-Methanolperylene (PeOH) was purchased from MicroChemistry Ltd. and used as received. *N*,*N*′-Dimethylaniline (DMA) was distilled at reduced pressure (3 Torr) under N_2 atmosphere (60 °C). Its purity was controlled by measurement of the refractive index. Proprionitrile, valeronitrile, octanenitrile, and decanenitrile were purified as described in the literature.[38] Toluene, chlorobenzene (CB), and the alkanes were of the highest commercially available purity and were used as such. Unless specified, all compounds were from Fluka.

For up-conversion measurements, the samples were placed in a rotating cell of 0.4 mm optical path length. The concentration of the samples was adjusted to obtain an absorbance at 400 nm of 0.1−0.15 on 0.4 mm. This corresponds to concentrations of $(2-3) \times 10^{-4}$ M.

For OHPS measurements, a similar concentration was used. The sample solutions were placed in a 1 mm thick quartz flow cell (Hellma). All measurements were carried out at 20 °C. All the solutions were bubbled with Ar for 15−20 min before use. The presence of oxygen had no influence on the fluorescence dynamics in DMA. On the other hand, the fluorescence lifetimes in inert solvents listed in Table 1 might be somewhat influenced by imperfect deoxygenation of the solutions. However, the remaining oxygen should not affect these values by more than 10%.

Fluorescence Data Analysis. Time-resolved fluorescence data were analyzed by iterative reconvolution of the instrument response function with trial functions (sum of exponentials) using a nonlinear least-squares fitting procedure (MATLAB, The MathWorks, Inc.). For most samples, measurements were carried out at three different wavelengths (438, 475, and 490 nm) and over several, typically five time scales, to accurately cover the span of the fluorescence decay. Global fits were done with all the available data. The goodness of the fit was evaluated by visual inspection of the residuals. A situation requiring special treatment was the analysis of the fluorescence rise due to vibrational relaxation processes. This ultrafast rise (100−300 fs depending on the wavelength) could not be reproduced with a sum of exponentials. Due to the difficulty to find a simple mathematical expression to describe this rise, the fitting range was limited to the fluorescence decay. This restriction may introduce some additional uncertainty on the analysis of decay components shorter than about 700 fs.

Results

Steady-State Measurements. The UV−vis absorption spectra of the acceptors in DMA are very similar to those measured in inert solvents. No additional band that could be ascribed to the formation of a complex can be observed. The fluorescence spectra of PeMe in CB and DMA are shown in Figure 1. CB was chosen because both its static dielectric constant ($\epsilon_s = 5.6$) and refractive index ($n = 1.524$) are similar to those of DMA ($\epsilon_s = 5.0$, $n = 1.558$).[21,39] In CB, the spectrum is due to the emission from the locally excited-state S_1 of PeMe. In DMA, these bands have almost totally vanished and are replaced by a broad and structureless spectrum centered at 570 nm that can be ascribed to the PeMe/DMA exciplex emission. Similar spectra are observed with the other acceptors. Figure 2 shows the fluorescence spectra of Pe and PeCN in toluene and in CB. For both molecules, a small bathochromic shift is observed by going from toluene to CB. Pe is centrosymmetric and has thus not permanent dipole moment. On the other hand, AM1 calculations indicate a dipole moment of 4.2 D for PeCN. This semiempirical procedure has recently been shown to give reliable values of permanent dipole moments.[23] Therefore, the similar solvatochromism observed with Pe and PeCN is not related to the dipole−dipole interaction, but rather to a larger dispersion interaction in the more polarizable CB.[26] This indicates that the dipole moment of PeCN is essentially the same in both ground and S_1 states. The same conclusion can be drawn for PeOH and PeMe.

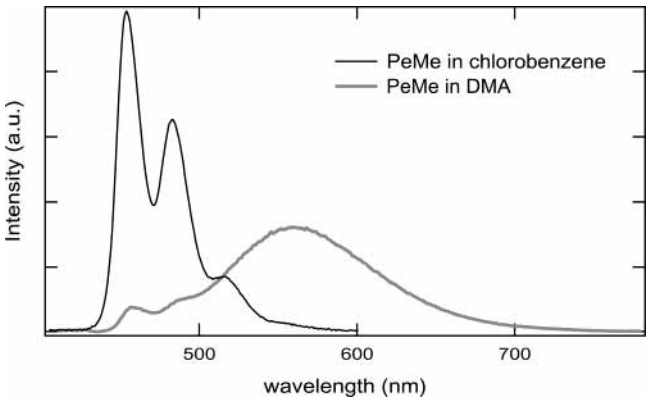

Figure 1. Steady-state fluorescence spectrum of PeMe in CB and in DMA. The relative intensity of the two spectra is arbitrary.

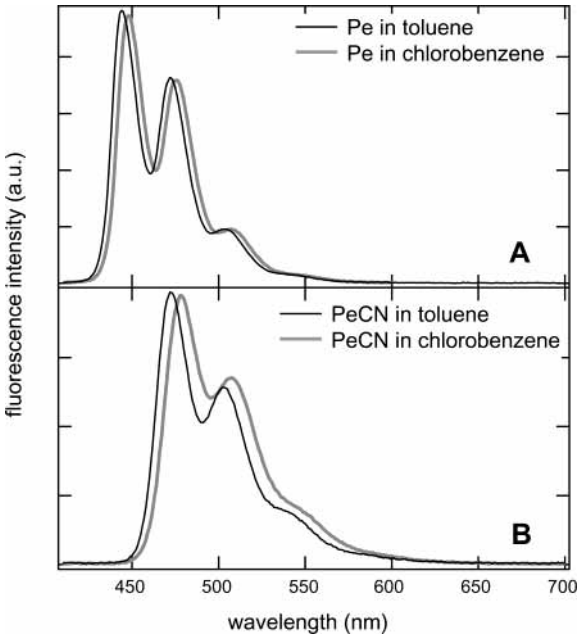

Figure 2. Steady-state fluorescence spectra of Pe (A) and PeCN (B) in toluene and in CB.

Fluorescence Up-Conversion Measurements. Before investigating the quenching dynamics in DMA, the fluorescence dynamics of Pe and PeCN was investigated in nonreacting solvents. Figure 3 shows the early fluorescence dynamics of Pe in toluene after 400 nm excitation. At wavelengths located at the wings of the fluorescence band, a decay component with

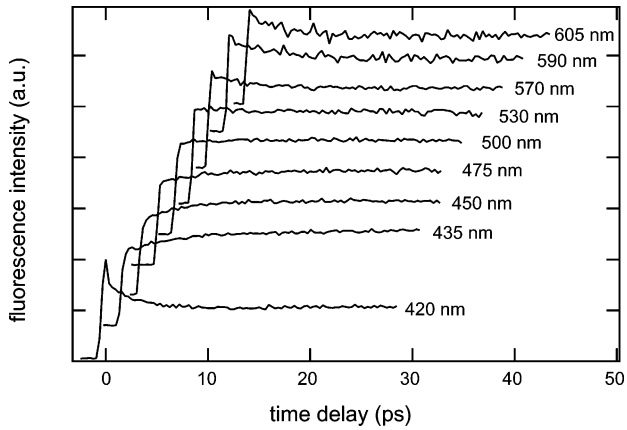

Figure 3. Early fluorescence dynamics of Pe in toluene at different wavelengths.

a time constant of 2.4 ps can be observed. After this initial decay, the fluorescence intensity decreases exponentially with a time constant of 4.4 ns, which corresponds to the excited-state lifetime of Pe. In this region, the rise of the fluorescence intensity is limited by the instrument response. At wavelengths located in the center of the emission band, this rise is biphasic with a slower component, which can be reasonably reproduced by a single exponential function with a 2.4 ps time constant. The faster rising component is markedly slower than the instrument response and cannot be reproduced by a single or a double exponential function (see the Experimental Section). This early dynamics cannot be ascribed to solvation, since Pe is nonpolar. The 2.4 ps component, which corresponds to a narrowing of the emission band, as well as the faster rising component can be attributed to vibrational energy relaxation, most probably to vibrational cooling.[40,41] A qualitatively similar behavior was observed with Pe in CB as well as with the other acceptors, the main difference being that with PeCN the emission band is red-shifted. This early dynamics will be discussed in more detail in a subsequent paper.

To minimize the interference with the quenching dynamics, time-resolved fluorescence measurements with Pe, PeCN, PeOH, and PeMe in DMA were carried out at wavelengths where the effect of vibrational relaxation on the fluorescence dynamics is the smallest. In this range, i.e., from 460 to 490 for Pe, PeOH, and PeMe and between 470 and 500 nm for PeCN, no significant wavelength dependence of the fluorescence decay in DMA was observed. At longer wavelengths, the contribution of the exciplex becomes visible.

As shown in Figure 4, the fluorescence time profiles of the perylene derivatives in DMA are highly nonexponential. They can be reproduced by a sum of at least two or three exponential functions or by a stretched exponential function.[42] The parameters obtained from a triexponential fit are collected in Table 2 together with the average lifetime

$$\tau_{av} = \frac{1}{I_0}\int_0^\infty I(t)\mathrm{d}t \qquad (2)$$

where $I(t)$ is the time dependent fluorescence intensity and I_0 is the maximum fluorescence intensity.

In DMA, the rise of the fluorescence and well as the maximum intensity were similar to those in toluene and CB. This precludes the occurrence of significant quenching components faster than the time resolution of the setup.

OHPS Measurements. Figure 5 shows the time profile of the pure heterodyne signal measured at 400 nm with PeMe in hexane. Apart from the first few ps (vide supra), the signal intensity decays exponentially to zero with a lifetime τ_H. A similar behavior is observed in series of *n*-alkanes and *n*-alkanenitriles of increasing viscosity. As the ground-state recovery dynamics of PeCN and PeMe can be expected to be exponential with a time constant equal to the fluorescence lifetime, τ_{fl}, it appears from eq 1 that $r(t)$ is exponential as well with a lifetime given by

$$\tau_r^{-1} = \tau_H^{-1} - \tau_{fl}^{-1} \cong \tau_H^{-1} \qquad (3)$$

In the present case, the decay of the anisotropy occurs through reorientational diffusion of the molecules. The reorientational times, τ_r, measured with PeCN and PeMe in various inert

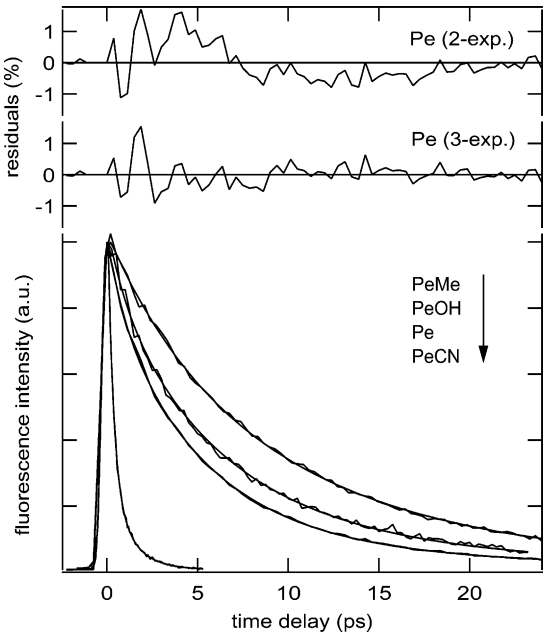

Figure 4. Time profiles of the fluorescence at 475 nm of Pe, PeCN, PeOH, and PeMe in DMA and best triexponential fits. For each fluorescer, the fit has been performed globally with several sets of data (see text). The residuals of the global fit of the Pe data assuming two- and three-exponential decay are shown in the upper panels.

TABLE 2: Amplitudes, A_i, and Time Constants, τ_i, Obtained from a Triexponential Fit to the Fluorescence Time Profiles of the Acceptors in DMA and Average Lifetime, τ_{av}

acceptor	A_1	τ_1 (ps)	A_2	τ_2 (ps)	A_3	τ_3 (ps)	τ_{av} (ps)
Pe	0.11	13.3	0.66	4.9	0.23	0.87	4.9
PeCN	0.01	2.5	0.13	.97	0.86	0.30	0.42
PeOH	0.24	12.0	0.56	5.4	0.20	1.0	6.1
PeMe	0.68	11.4	0.32	4.7	-	-	9.3

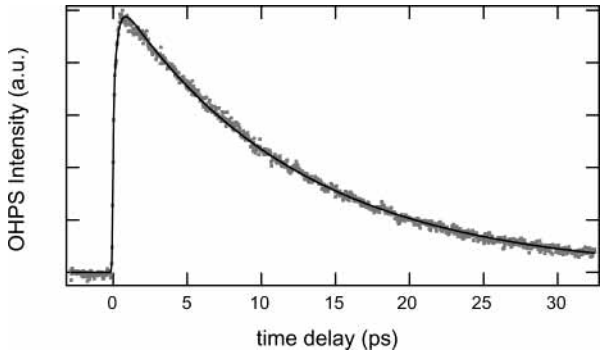

Figure 5. Time profile of the OHPS signal measured with PeMe in hexane.

TABLE 3: Reorientational Times, τ_r, of PeCN and PeMe in Different Classes of Solvents (Error on τ_r: ±4%)

solvent	η (cP)	τ_r (PeCN) (ps)	τ_r (PeMe) (ps)
pentane	0.235	11.0	9.8
hexane	0.313	14.7	11.8
heptane	0.418	17.3	13.4
decane	0.928	31.5	25
dodecane	1.51	47	37
acetonitrile	0.35	18.8	14.5
propionitrile	0.41	22	17.5
valeronitrile	0.74	39	27
octanenitrile	1.64	81	41
decanenitrile	2.66	131	68

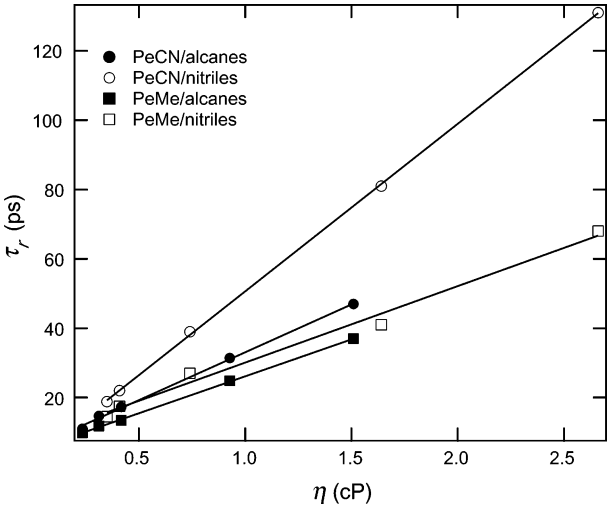

Figure 6. Viscosity dependence of the reorientational time of PeCN and PeMe in alkanes and in nitriles.

solvents are listed in Table 3. These two molecules can be described as oblate ellipsoids with the transition dipole moment perpendicular to the molecular (short) axis. In this case, the decay of the anisotropy should in principle be biexponential.[34,43] However, the experimentally observed decays can in most cases, as here, be reproduced with a single-exponential function. The observed time constants, τ_r, are generally discussed in terms of a modified Stokes−Einstein−Debye equation[34,44]

$$\tau_r = \frac{fVC\eta}{k_B T} \tag{4}$$

where f is a shape factor[34,45] that depends on the axis ratio of the ellipsoid and can be estimated to be around 1.35 for PeCN and PeMe, V is the volume of the rotating body, η is the solvent viscosity, and C is the boundary condition parameter. The latter amounts to 1 for stick hydrodynamics, i.e., when molecules of the first solvent shell follow the reorientational motion of the solute. This condition is often found with polar molecules in polar solvents,[46−48] i.e., in cases where dipole−dipole interaction is operative. For slip hydrodynamics, the value of C depends on the axis ratio of the rotating ellipsoid. For a spherical body, $C = 0$; i.e., the molecule rotates freely and independently of the surrounding solvent. For molecules such as PeCN and PeMe, with an axis ratio of about 0.45, C should amount to 0.3.[49]

Figure 6 shows that for a given solute and a given class of solvent, τ_r increases linearly with viscosity. The corresponding slopes and the boundary parameters C are listed in Table 4. It appears that for PeMe the viscosity dependence of τ_r is the same in both polar and nonpolar solvents. The parameter C indicates slip hydrodynamics; i.e., the rotational motion of PeMe requires only the neighbor solvent molecules to be pushed away. The larger the departure of PeMe from a sphere, the larger C. Essentially the same behavior is observed with PeCN in the alkanes. The situation changes substantially with PeCN in polar solvents, where the slope, hence C, is about twice that in nonpolar solvents. This difference can be ascribed to the effect of dielectric friction,[33,50,51] which is absent with the other solute/solvent systems.

TABLE 4: Slopes and Intercepts Obtained from the Linear Fit of eq 4 to the Measured Viscosity Dependence of the Reorientational Time of PeCN and PeMe in Different Classes of Solvents

solute/solvent	slope (ps/cP)	intercept (ps)	C
PeCN/alkanes	27.6	5.4	0.34
PeMe/alkanes	21.3	4.8	0.28
PeCN/nitriles	48.3	2.0	0.61
PeMe/nitriles	22.0	8.0	0.29

On the other hand, the intercept is different from zero but does not change significantly. Its physical meaning has been discussed in detail in ref 52.

Discussion

Data Analysis. The fluorescence decays of Pe and derivatives in DMA are strongly nonexponential. This reflects a distribution of quenching rate constants due to a distribution of distinct arrangements of the DMA molecules around the acceptor. In general, distributions of exponentials can be well reproduced with bi- or three exponential functions, but these exponentials do not give direct physical insight.[53] In an attempt to reproduce these decays while accounting for these distributions, we have elaborated a simple model. This model assumes that ET occurs only with donors from the first solvent shell. Moreover, on the basis of the molecular dynamics simulations of Castner et al.,[21] only a few molecules of this first shell are assumed to be in an optimal position for ET. The others need first some rotational and/or translational diffusion before reaching such a position. Therefore, the donor molecules can be sorted into three classes: donors that are in an optimal position to quench the acceptor molecules (D_a), donors that have first to rotate (D_b), and donors that need translational motion (D_c). All D_a molecules undergo ET with a rate constant, which is certainly not unique, but which is larger than those for rotational and translational diffusion. Nevertheless, we assume for simplicity a single ET rate constant, k_{ET}, for the D_a molecules. For the other groups, ET is rotational or translational diffusion controlled and thus proceeds with a rate constant k_R and k_T, respectively, because $k_T \ll k_R \ll k_{ET}$. Hence, the rate constant, k_i, for the fluorescence decay of an acceptor with a given solvent configuration i is the sum of the individual ET rate constants with the donors of the first solvent shell

$$k_i = n_{ai}k_{ET} + n_{bi}k_R + n_{ci}k_T + k_{fl} \tag{5}$$

where n_{ai}, n_{bi} and n_{ci} are the number of D_a, D_b, and D_c molecules in the solvent configuration i around an acceptor and k_{fl} is the fluorescence rate constant without quenching. Since there are $N = (n + 2)!/(n!2!)$ possible arrangements of n donors, each one with different n_a, n_b, and n_c, the overall fluorescence decay consists of a distribution of exponentials, in agreement with the nonexponential kinetics observed here and in other investigations.[10,11,14,15,21]

All the possible arrangements of donors are not equally probable. The probability for a given arrangement P_i to be realized depends on the number n of donor molecules in the first shell, $n = n_a + n_b + n_c$, and on P_a, P_b, and P_c, the

probabilities for a donor molecule to be a D_a, D_b, or D_c, respectively:[54,55]

$$P_i = \frac{n!}{n_{ai}!n_{bi}!n_{ci}!}P_a^{n_{ai}}P_b^{n_{bi}}P_c^{n_{ci}} \quad (6)$$

Once P_i and k_i obtained for each of the N possible arrangements, the fluorescence kinetics, $I(t)$, can be computed by summing over all the possible exponential decays weighted according to their probability:

$$I(t) = \sum_{i=1}^{N} P_i \exp(-k_i t) \quad \text{with} \quad \sum_{i=1}^{N} P_i = 1 \quad (7)$$

At this point, we have a model and the equations required to simulate the data, but the parameters n, k_{ET}, k_R, k_T, P_a, and P_b ($P_c = 1 - P_a - P_b$) are not known. Some of them, n, k_R, and k_T, can be obtained through calculations or measurements. As these three parameters depend mainly on the solvent, they should be constant for the four acceptors investigated here. The remaining parameters, k_{ET}, P_a, and P_b, depend mostly on the nature of the acceptor and cannot be obtained so readily. The different dynamics measured with the various acceptor/DMA systems, although very similar from the energetic point of view (see next section and Table 1), should most probably be reflected by differences in these three latter parameters. To check the validity of this model and to obtain some estimates of k_{ET}, P_a, and P_b, eq 7 was fitted to the experimental data. For the fit, n, k_R, and k_T were kept constant while k_{ET}, P_a, and P_b were adjusted.

For the estimation of n, the molecular volumes of DMA, $V_{DMA} = 127.7$ Å^3, and of Pe, $V_{Pe} = 225.6$ Å^3, were first determined using the van der Waals increments method.[56] Then, assuming spherical molecules with radii $r_{DMA} = 3.12$ Å and $r_{Pe} = 3.78$ Å, a volume of 4219.3 Å^3 was calculated for the sphere of radius $r = 10.02$ Å enclosing one Pe molecule with the first solvent shell. To deduce the number of DMA molecules contained in this volume and to take the interstitial volume into account,[56] Pe and DMA were considered as cubes with sides equal to $2r_{Pe}$ and $2r_{DMA}$, respectively. This approach results to a value of $n = 16$. As a test of reliability, the number of DMA molecules around coumarin 152, already determined by molecular dynamics simulation,[21] was also estimated with this method. The obtained value, about 15 molecules in the first solvent shell, is indeed in excellent agreement with that of 13−16 molecules from the simulation. Therefore, although rough, this method seems quite efficient to obtain a good estimate of n, at least for these systems.

The rate constant of rotational diffusion of the donor, k_R, was taken as the inverse dielectric relaxation time of DMA measured by microwave absorption.[57]

The rate constant of translational diffusion, k_T, was calculated using the following equation[58]

$$k_T = \frac{D_T}{j^2} \quad (8)$$

where j, the distance between two equilibrium positions of a DMA molecule, was taken as $2r_{DMA}$. The translational diffusion coefficient, D_T, was calculated from the Stokes−Einstein equation

$$D_T = \frac{k_B T}{6\pi r \eta} \quad (9)$$

where r is the radius of the diffusing molecule.

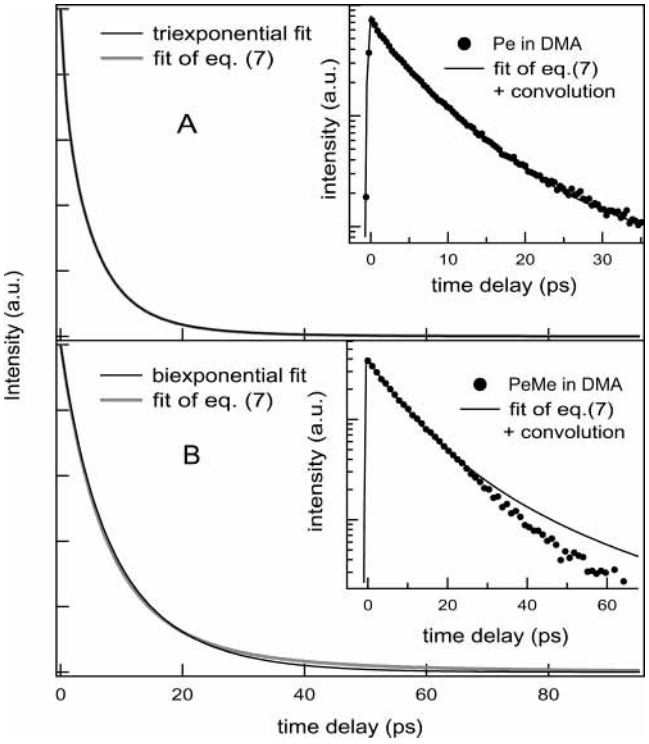

Figure 7. Comparison of the best fit of eq 7 with the triexponential function reproducing the decay of Pe (A) and PeMe (B) fluorescence in DMA (see text for details). Inset: comparison of the best fit of eq 7, after reconvolution with the instrument response function, with the experimental data.

TABLE 5: Parameters Obtained from the Fit of eq 7 to the Fluorescence Decay of the Acceptors in DMA[a]

acceptor	n	τ_{ET} (ps)	P_a	P_b	n_a	n_b
Pe	11	1.2	0.025	0.435	<1	5
	16	1.1	0.016	0.303	<1	5
	21	1.1	0.011	0.226	<1	5
PeCN	11	1.2	0.309	.655	3−4	7
	16	1.3	0.232	.476	3−4	8
	21	1.4	0.185	.368	3−4	8
PeOH	11	1.1	0.0175	0.381	<1	4
	16	1.1	0.011	0.260	<1	4
	21	1.1	0.0085	0.191	≪1	4
PeMe	11	-	-	0.305	-	3
	16	-	-	0.200	-	3
	21	-	-	0.143	-	3

[a] Number of molecules in the first solvent shell, n, time constant of ET for optimal orientation, τ_{ET} (=$1/k_{ET}$), average number of donor molecules with optimal orientation, n_a, or requiring reorientation, n_b, and related probabilities, P_a and P_b.

Using n, k_R, and k_T as constants, eq 7 was fitted to the experimental data using a nonlinear least-squares method. To simplify the procedure, it was more convenient to use the best multiexponential functions obtained from the data analysis (see Table 2) instead of the measured data. In this way, several procedures, such as background noise correction, reconvolution, and global analysis, that strongly slow the fit could be avoided. To test the sensitivity of the model to n, the fit was also carried out with $n \pm 5$ donor molecules in the first solvent shell.

The results from this fitting/simulation are surprisingly good for such a simple model. Figure 7A shows that the best multiexponential fit to the decay of Pe fluorescence is well reproduced by eq 7. A similar agreement was found with PeCN and PeOH. The best fit parameters listed in Table 5 show some very interesting trends. The ET rate constant, k_{ET}, is practically the same for Pe, PeCN, and PeOH. Their different quenching

dynamics, especially for PeCN, is essentially due to different arrangements of donors, i.e., to their different probabilities of having a donor molecule in an optimal position for ET (P_a). For PeCN, P_a is high, and this molecule is on average surrounded by 3−4 D_a molecules ($n_a = P_a n$). On the other hand, P_a is much lower for Pe and PeOH. This implies that for more than 70% of the acceptor molecules some diffusional motion of the donors must occur before quenching. Repeating the fit of eq 7 to the data with PeCN by forcing either P_a to be the same as for Pe or τ_{ET} to be shorter (400 fs) does not result at all to a good agreement with the data.

PeMe exhibits a different behavior: its best multiexponential decay function is not so well reproduced as in the former cases, especially at long times (see Figure 7B). The best fit parameters show that the number of D_a molecules is too small to affect the decay dynamics. This is consistent with the absence of a fast fluorescence decay component for this acceptor (see Table 2).

Finally, Table 5 shows that the value of n has no marked influence on k_{ET}, n_a, and n_b.

Influence of the Solute−Solvent Interactions on the Quenching Dynamics. According to the model described above, the much faster quenching dynamics measured with PeCN compared to the other acceptors is not due to a larger ET rate constant for the PeCN/DMA system, but essentially to a larger number of donor molecules with an optimal position for ET. This result is totally consistent with the rather similar ET driving force for these systems. Indeed, according to ET theories, a 0.1 eV increase in driving force in the exergonic region could at most account for a 2−3-fold increase of the ET rate constant.

As mentioned in the Introduction, the major difference between Pe and PeCN is the polarity. The dipole moment of PeCN in the ground state determined by AM1 calculations amounts to 4.2 D. This dipole points from the aromatic ring toward the cyano group. As neither absorption nor fluorescence bands of PeCN shift with solvent polarity, the dipole moment does not change significantly in size and direction upon excitation. Because of this, the occurrence of dipole−dipole interaction of PeCN with the environment is not visible in the spectra. On the other hand, the electric dipole of DMA amounts to 1.61 D[21] and points from the amino-group toward the benzene ring. Therefore, dipole−dipole interaction should favor a mutual geometry where the aromatic planes of PeCN and DMA are face to face. As shown by the calculations of Castner et al.,[21] such a geometry can be expected to lead to a large electronic coupling constant and, hence, to a fast ET. Of course, at room temperature the solute−solvent orientations fluctuate very rapidly, but the dipole−dipole interaction should limit the degree of freedom of the donor molecules surrounding PeCN. In other words, this interaction should lead to an enhancement of the number of D_a molecules. This is supported by the measurement of the reorientational dynamics of PeCN and PeMe presented above. The markedly larger boundary value, C, measured with PeCN in polar solvents compared to nonpolar solvents and to the very weakly polar PeMe, is a direct manifestation of the dipole−dipole interaction, leading to an additional frictional term between the solute and the solvent.

The main interactions between the nonpolar Pe and DMA are $\pi-\pi$ interactions. They have been shown to favor several mutual orientations, such as those where the aromatic planes are edge-to-face or are parallel but shifted.[59] In these orientations, the electronic coupling can be expected to be substantially smaller than in the face-to-face one. However, the latter geometry is not favored by $\pi-\pi$ interactions because of a larger electrostatic repulsion. Therefore, the number of D_a molecules around Pe should be substantially smaller than around PeCN, in agreement with the results of the above analysis.

The calculated electric dipole moment of PeOH is substantially smaller than that of PeCN, about 2 D, and points out of the aromatic plane. Moreover, H bonding to the lone pair on the nitrogen atom of DMA is possible. Our analysis indicates that the number of D_a molecule around PeOH is similar to that around Pe, despite both dipole−dipole and H-bonding interactions. The insensitivity of the quenching dynamics on the H-bonding could be explained by a rather large distance of the two aromatic planes in the H-bound complex. Therefore, this interaction should not enhance electronic coupling. The same may happen with the dipole−dipole interaction. First, this interaction is weaker than with PeCN and second as the electric dipole moment is not in the aromatic plane contrarily to PeCN, the arrangements favoring dipole−dipole interaction should not be those where the electronic coupling is the highest.

The slowest quenching dynamics was found with PeMe. As shown in Table 2, the ultrafast decay component observed with the other acceptors is absent with PeMe. The analysis according to the three-donor types model indicates a number of D_a molecules close to zero. As first sight, one would have predicted a behavior very similar to that of Pe. One could nevertheless invoke two effects that, if really operative, could only lead to a deterioration of the electronic coupling. The first one is the steric hindrance by the methyl group,[60−62] and the second one is the presence of a permanent dipole moment of about 0.5 D pointing from the methyl group toward the aromatic system, i.e., in the opposite direction to that of PeCN. Therefore, contrary to PeCN, the interaction of this dipole with that of DMA should favor a mutual geometry where the aromatic planes of the two reactants are not face-to-face.

It is interesting to note that although the driving force for ET is essentially the same for Pe and PeMe, the energy difference between the local and exciplex fluorescence band maxima is larger by about 0.07 eV with Pe. The origin of this difference might be related to structural differences of the Pe/DMA and PeMe/DMA exciplexes, which may reflect different mutual orientations of the reactants. Computer modeling of the influence of substitution on the perylene/DMA geometry is planned.

Figure 7B shows that the three-donor types model does not reproduce the observed fluorescence decay of PeMe as well as with the other acceptors. This discrepancy most probably originates from the crude description of the translational diffusion process. For Pe, PeCN, and PeOH, a poor estimation of k_T has essentially no effect on the quality of the fit to the data. Indeed, with these acceptors, essentially the whole quenching is due to D_a and D_b molecules, and therefore, the D_c molecules are essentially inactive. This is no longer the case with PeMe, whose quenching seems to involve D_c molecules as well. If the fit is performed by letting τ_T ($= k_T^{-1}$) free, the data can be well reproduced with a τ_T of about 300 ps instead of the 800 ps obtained from eqs 8 and 9. Equation 9 is known to underestimate the translational diffusion coefficient, D_T.[56] If the latter is calculated with the semiempirical expression of Spernol and Wirtz,[63] a τ_T value of 410 ps is obtained, in much better agreement with the best fit value.

Comparison between Tables 2 and 5 shows that for Pe and PeOH, the time constant of the fast decay component, τ_3, is close to the τ_{ET} value obtained from the above model. This is due to the fact that, for these two acceptors, the probability of having more than one D_a molecule is essentially zero. Therefore, the fastest decay component of Pe and PeOH fluorescence is

due to the arrangements with one D_a molecule. For those cases, the faster quenching component gives a good estimate of the ET time constant. This is no longer the case with PeCN, for which the faster quenching component is due to arrangements with typically four D_a molecules. For these arrangements, $\tau_{ET} \approx 4\tau_3$, and thus, the ET time constant cannot be directly deduced from the faster quenching component.

These results agree well with the conclusion of the molecular dynamics investigation of Castner et al.[21] that at a given instant there are 2−5 DMA molecules with a large electronic coupling around coumarin 152. The coumarins that have been intensively used as acceptors in electron donating solvents are characterized by a large permanent dipole moment in the electronic ground state,[23] and therefore, dipole−dipole interaction can be expected to influence the mutual donor−acceptor orientation as found here with PeCN. The ET quenching dynamics in DMA has also been investigated with ionic acceptors, such as Nile Blue, Oxazine 1, and Rhodamine 6G, in DMA. In these cases as well, the donor−acceptor mutual orientation, hence the electronic coupling, must be influenced by the electrostatic interactions.

Absolute Value of τ_{ET}. Although the τ_{ET} value found using the above model is substantially larger than that reported for Oxazine 1 in DMA,[11] it is astonishingly small for a such a weakly exergonic ET. The solvation dynamics of DMA is rather complex as reported by Yoshihara, Meech, and co-workers.[64−67] Solvation occurs essentially by diffusional motion with time constants of 3.8 ps (35%) and 22.6 ps (65%). Optical Kerr effect measurements indicate that 10−20% of the total solvent response occur during the first 200 fs via inertial motion.[64] However, this contribution was not found in fluorescence dynamic Stokes shift measurements.[67] Therefore, the ET time constants found here with Pe, PeCN, and PeOH are substantially smaller than the time scales of diffusive solvation. Theoretically, this situation can be discussed in terms of the classical two-dimensional Sumi−Marcus model.[68−70] In this model, one can define, for each position of the system along the solvent coordinate, X, an ET rate constant, $k_{ET}(X)$, X decreasing from 1 to zero in time scales specific to the solvent. Therefore, the effective driving force and solvent reorganization energy for ET are functions of X

$$\Delta G_{ET}(X) = \Delta G_{ET} + X\lambda_s \quad \text{and} \quad \lambda_s(X) = (1 - X)\lambda_s \quad (10)$$

where ΔG_{ET} and λ_s are the equilibrium driving force and solvent reorganization energy. These two equations can be inserted into the Marcus expression for nonadiabatic ET reaction to obtain $k_{ET}(X)$.[71,72]

The time evolution of the excited-state population was calculated as described in ref 73, using a biexponential decay with the solvation time constants mentioned above to model the evolution along X for DMA, with $\lambda_s = 0.45$ eV, $\Delta G_{ET} = -0.18$ eV and an intramolecular reorganization energy of $\lambda_i = 0.28$ eV.[74] To reproduce an effective time constant of 1 ps, an electronic coupling constant of $V = 800$ cm^{-1} had to be used. This value is very large, and certainly above the limit of validity of the nonadiabatic ET theory.[72,75] Nevertheless, it is not totally inconsistent with those calculated by Castner et al. for coumarin 152 in DMA. Among the 15 DMA molecules surrounding an acceptor, three donors were found to have a coupling constant superior to 200 cm^{-1}, namely 266, 566, and 779 cm^{-1}.[21]

A similar population decay with a smaller V can be obtained by using a smaller initial value of X or alternatively by introducing an ultrafast inertial component in the decay of X. However, the latter assumption is not supported by fluorescence Stokes shifts measurements.[67] A smaller initial X would physically corresponds a solvent configuration partially oriented for ET. In the ET time scale found here, diffusive solvent motion is frozen and there is a large distribution of solvent configurations around the excited acceptors. Statistically, these distributions are centered on an X value of 1. However, some of these configurations must correspond to $X < 1$. Consequently, the ultrafast quenching component measured in this investigation may be due to the fraction of the acceptor population with a donor molecule at the right position for large electronic coupling but with *additionally* an appropriate solvent configuration. This constraint on "presolvation" may be larger with Pe, PeOH, and PeMe, for which the ET driving force is the smallest. This could be an additional reason for the much smaller n_a value with these acceptors. The rate constant k_R may account for an ET limited by the reorientation of the donor molecules not only for a better coupling but also for a better solvation, i.e., a smaller X.

Finally, exciplex emission has been observed with all the acceptors investigated here. The dynamics of the quenching product will be discussed in detail in a forthcoming paper. This observation implies that the degree of charge transfer, although large, is not full. Moreover, the effective driving force for quenching might be larger than that for full ET, due to an additional stabilization energy of the exciplex.[24] Consequently, one should be cautious when using nonadiabatic ET theory for discussing such systems.

Concluding Remarks

A major advantage of the acceptors investigated here over those used in other studies in electron-donating solvents is their structural simplicity and the possibility to tune the solute−solvent interactions without affecting too much the other properties. This has given the possibility to emphasize the effect of these interactions on the quenching dynamics. The three-donor types model proposed here is crude but accounts for the whole, strongly nonexponential, decay of the excited acceptor population. The values of the resulting parameters must not be taken too literally, but must be considered as indicative. This model can of course be refined with better descriptions of the diffusional motion. However, we think that a significant improvement can only be achieved by a combination of molecular-dynamics simulations and ET rate calculations/fit performed on a large ensemble of excited acceptors.

According to our investigation, one should be very careful when identifying the quenching rate constant measured in pure donating solvents or at high quencher concentration with the rate constant of bimolecular ET. This assumption was found to be valid with Pe and PeOH but not with PeCN.

This investigation shows that the dipole−dipole interaction between the reactants can affect the dynamics of a bimolecular ET reaction. Until now, this effect has been largely neglected. Preliminary measurements in a nonpolar solvent indicate that this interaction can lead to an enrichment of a polar quencher concentration around a polar excited reactant. This results to an enhancement of the so-called transient effect. In this case, a Collins−Kimball analysis results to an overestimation of the critical distance and of the reaction rate constant. Further measurements on this effect are in progress.

Acknowledgment. We wish to thank Dr. P. Rosa and Mr. C. Gouverd for their assistance in electrochemical measurements as well as Mr. O. Nicolet and Mr. A. Pigliucci for the TCSPC measurements. This work was supported by the Fonds National Suisse de la Recherche Scientifique through Project No. 2000-0632528.00.

References and Notes

(1) Rehm, D.; Weller, A. *Isr. J. Chem.* **1970**, *8*, 259.
(2) Nishikawa, S.; Asahi, T.; Okada, T.; Mataga, N.; Kakitani, T. *Chem. Phys. Lett.* **1991**, *185*, 237.
(3) Murata, S.; Tachiya, M. *J. Chem. Phys.* **1996**, *93*, 1577.
(4) Jacques, P.; Allonas, X. *Chem. Phys. Lett.* **1995**, *233*, 533.
(5) Scully, A. D.; Takeda, T.; Okamoto, M.; Hirayama, S. *Chem. Phys. Lett.* **1994**, *228*, 32.
(6) Swallen, S. F.; Weidemaier, K.; Fayer, M. D. *J. Chem. Phys.* **1996**, *104*, 2976.
(7) Gladkikh, V. S.; Burshtein, A. I.; Tavernier, H. L.; Fayer, M. D. *J. Phys. Chem. A* **2002**, *106*, 6982.
(8) Murata, S.; Nishimura, M.; Matsuzaki, S. Y.; Tachiya, M. *Chem. Phys. Lett.* **1994**, *200*, 219.
(9) Kakitani, T.; Matsuda, N.; Yoshimori, A.; Mataga, N. *Prog. React. Kinet.* **1995**, *20*, 347.
(10) Kobayashi, T.; Tagaki, Y.; Kandori, H.; Kemnitz, K.; Yoshihara, K. *Chem. Phys. Lett.* **1991**, *180*, 416.
(11) Rubstov, I. V.; Shirota, H.; Yoshihara, K. *J. Phys. Chem. A* **1999**, *103*, 1801.
(12) Yoshihara, K.; Tominaga, K.; Nagasawa, Y. *Bull. Chem. Soc. Jpn.* **1995**, *68*, 696.
(13) Yoshihara, K. Ultrafast Intermolecular Electron Transfer in Solution. In *Electron Transfer*: *From Isolated Molecules to Biomolecules*; Jortner, J., Bixon, M., Eds.; John Wiley: New York, 1999; Vol. 107; p 371.
(14) Engleitner, S.; Seel, M.; Zinth, W. *J. Phys. Chem. A* **1999**, *103*, 3013.
(15) Xu, Q.-H.; Scholes, G. D.; Yang, M.; Fleming, G. R. *J. Phys. Chem. A* **1999**, *103*, 10348.
(16) Tannor, D.; Rice, S. A. *J. Chem. Phys.* **1985**, *93*, 5013.
(17) Brumer, P.; Shapiro, M. *Chem. Phys. Lett.* **1986**, *126*, 541.
(18) Assion, A.; Baumert, T.; Helbing, J.; Seyfried, V.; Gerber, G. *Chem. Phys. Lett.* **1996**, *259*, 488.
(19) Bardeen, C. J.; Che, J.; Wilson, K. R.; Yakovlev, V. V.; Cong, P.; Kohler, B.; Krause, J. L.; Messina, M. *J. Chem. Phys.* **1997**, *101*, 3815.
(20) Scherer, P. O. J. *J. Phys. Chem. A* **2000**, *104*, 6301.
(21) Castner, E. W., Jr.; Kennedy, D.; Cave, R. J. *J. Phys. Chem. A* **2000**, *104*, 2869.
(22) Baigar, E.; Gilch, P.; Zinth, W.; Stöckl, M.; Härter, P.; von Feilitzsch, T.; Michel-Beyerle, M. E. *Chem. Phys. Lett.* **2002**, *352*, 176.
(23) Cave, R. J.; Castner, E. W., Jr. *J. Phys. Chem. A* **2002**, *106*, 12117.
(24) Weller, A. *Z. Phys. Chem. N. F.* **1982**, *133*, 93.
(25) Siegerman, H. In *Techniques of Chemistry*; Weinberg, N. L., Ed.; John Wiley: New York, 1975; Vol. V; p 667.
(26) Suppan, P. *J. Photochem. Photobiol.* **1990**, *A50*, 293.
(27) Muller, P.-A.; Högemann, C.; Allonas, X.; Jacques, P.; Vauthey, E. *Chem. Phys. Lett.* **2000**, *326*, 321.
(28) Morandeira, A.; Engeli, L.; Vauthey, E. *J. Phys. Chem. A* **2002**, *106*, 4833.
(29) Gumy, J.-C. Ph.D. Thesis, University of Fribourg, 2000.
(30) McMorrow, D.; Lotshaw, W. T.; Kenney-Wallace, G. *IEEE J. Quantum Electron.* **1988**, *24*, 443.
(31) Chang, Y. J.; Castner, E. W., Jr. *J. Chem. Phys.* **1993**, *99*, 113.
(32) Alavi, D. S.; Hartman, R. S.; Waldeck, D. H. *J. Chem. Phys.* **1990**, *92*, 4055.
(33) Hartman, R. S.; Konitsky, W. M.; Waldeck, D. H.; Chang, Y. J.; Castner, E. W., Jr. *J. Chem. Phys.* **1997**, *106*, 7920.
(34) Fleming, G. R. *Chemical Applications of Ultrafast Spectroscopy*; Oxford University Press: New York, 1986.
(35) Joo, T.; Jia, Y.; Yu, J.-Y.; Lang, M. J.; Fleming, G. R. *J. Chem. Phys.* **1996**, *104*, 6089.
(36) Gumy, J. C.; Nicolet, O.; Vauthey, E. *J. Phys. Chem. A* **1999**, *103*, 10737.
(37) Buu-Hoï, N. P.; Long, C. T. *Rec. Trav. Chim. Pays-Bas* **1956**, *75*.
(38) Perrin, D. D.; Armarego, W. L. F.; Perrin, D. R. *Purification of Laboratory Chemicals*; Pergamon Press: Oxford, 1980.
(39) Riddick, J. A.; Bunger, W. B. *Organic Solvents*; J. Wiley: New York, 1970.
(40) Schwarzer, D.; Hanisch, C.; Kutne, P.; Troe, J. *J. Phys. Chem. A* **2002**, *106*, 8019.
(41) Kovalenko, S. A.; Schanz, R.; Hennig, H.; Ernsting, N. P. *J. Chem. Phys.* **2001**, *115*, 3256.
(42) Edholm, O.; Blomberg, C. *Chem. Phys.* **1999**, *252*, 221.
(43) Tao, T. *Biopolymers* **1969**, *8*, 609.
(44) Debye, P. *Polar Molecules*; Dover: New York, 1929.
(45) Perrin, F. *J. Phys. Rad.* **1934**, *5*, 497.
(46) von Jena, A.; Lessing, H. E. *Ber. Bunsen-Ges. Phys. Chem.* **1979**, *83*, 3.
(47) Vauthey, E. *Chem. Phys. Lett.* **1993**, *216*, 530.
(48) Williams, A. M.; Jiang, Y.; Ben-Amotz, D. *Chem. Phys.* **1994**, *180*, 119.
(49) Hu, C. M.; Zwanzig, R. *J. Chem. Phys.* **1974**, *60*, 4354.
(50) Horng, M. L.; Gardecki, J. A.; Maroncelli, M. *J. Phys. Chem. A* **1997**, *101*, 1030.
(51) Dutt, G. B.; Raman, S. *J. Chem. Phys.* **2001**, *114*, 6702.
(52) Evans, G. T.; Kivelson, D. *J. Chem. Phys.* **1986**, *84*, 385.
(53) Siemiarczuk, A.; Wagner, B. D.; Ware, W. R. *J. Phys. Chem.* **1990**, *94*, 1661.
(54) Young, H. D. *Statistical Treatment of Experimental Data*; McGraw-Hill: New York, 1962.
(55) Bevington, P. R. *Data Reduction and Error Analysis for the Physical Sciences*; McGraw-Hill: New York, 1969.
(56) Edward, J. T. *J. Chem. Educ.* **1970**, *4*, 261.
(57) Garg, S. K.; Smyth, C. P. *J. Chem. Phys.* **1967**, *46*, 373.
(58) Glasstone, S.; Laidler, K.; Eyring, H. *Theory of Rate Processes*; McGraw-Hill: New York, 1941.
(59) Hunter, C. A.; Sanders, J. K. M. *J. Am. Chem. Soc.* **1990**, *112*, 5525.
(60) Kluge, T.; Brede, O. *Chem. Phys. Lett.* **1998**, *289*, 319.
(61) Rathore, R.; Lindeman, S. V.; Kochi, J. K. *J. Am. Chem. Soc.* **1997**, *119*, 9393.
(62) Vauthey, E. *J. Phys. Chem.* **2000**, *104*, 1804.
(63) Spernol, A.; Wirtz, K. *Z. Naturforschung* **1953**, *8a*, 522.
(64) Smith, N. A.; Lin, S.; Meech, S. R.; Shirota, H.; Yoshihara, K. *J. Chem. Phys. A* **1997**, *101*, 9578.
(65) Smith, N. A.; Meech, S. R.; Rubstov, I. V.; Yoshihara, K. *Chem. Phys. Lett.* **1999**, *303*, 209.
(66) Smith, N. A.; Meech, S. R. *J. Phys. Chem. A* **2000**, *104*, 4223.
(67) Pal, H.; Nagasawa, Y.; Tominaga, K.; Kumazaki, S.; Yoshihara, K. *J. Chem. Phys.* **1995**, *102*, 653.
(68) Sumi, H. *J. Mol. Liquids* **1985**, *65/66*, 65.
(69) Sumi, H.; Marcus, R. A. *J. Chem. Phys.* **1986**, *84*, 4272.
(70) Sumi, H.; Marcus, R. A. *J. Chem. Phys.* **1986**, *84*, 4894.
(71) Walker, G. C.; Akesson, E.; Johnson, A. E.; Levinger, N. E.; Barbara, P. F. *J. Phys. Chem.* **1992**, *96*, 3728.
(72) Marcus, R. A.; Sutin, N. *Biochim. Biophys. Acta* **1985**, *811*, 265.
(73) Nicolet, O.; Vauthey, E. *J. Phys. Chem. A* **2002**, *106*, 5553.
(74) Vauthey, E. *J. Phys. Chem. A* **2001**, *105*, 340.
(75) Heitele, H. *Angew. Chem., Int. Ed. Engl.* **1993**, *32*, 359.